How fast can thiols bind to the gold-nanoparticle surface?

Amanda Bard, Rebeca Rondon, Daniela T. Marquez, Anabel E. Lanterna*, Juan C. Scaiano*

Department of Chemistry and Biomolecular Sciences, Centre for Advanced Materials Research (CAMaR), University of Ottawa, Ottawa, Ontario K1N 6N5, Canada

*Corresponding authors' e-mails: alantern@uottawa.ca (AEL) jscaiano@uottawa.ca (JCS)

ORCID numbers:

A.E. Lanterna: 0000-0002-6743-0940; J.C. Scaiano: 0000-0002-4838-7123

[a] Dedicated to Professor E.A. Lissi, as he reaches a new milestone.

ABSTRACT

Kinetics of gold-nanoparticle-surface modification with thiols can take more than one hour for completion. 7-Mercapto-4-methylcoumarin, can be used to follow the process by fluorescence spectroscopy and serves as a convenient molecular probe to determine relative kinetics of other thiol compounds. SERS studies with aromatic thiols further support the slow surface modification kinetics observed by fluorescence spectroscopy. The formation of thiolate bonds is a relatively slow process; we recommend one to two hour wait for thiol binding to be essentially complete, while for disulfides, overnight incubation is suggested.

INTRODUCTION

While there are numerous ways to stabilize gold nanoparticles (AuNP) the most common ones involve the formation of the thiolate S-Au bond (~130 kJ/mol), frequently by reaction of thiols with the gold surface (1). The modification of gold surfaces with thiol compounds has been extensively explored as one of the best gold surface passivation methods, as well as the best way to anchor different functional groups to the surface (1-6). While the strategy has proven thermodynamically effective and efficient, the complex kinetics of the reaction have been frequently overlooked. The process is well understood when it involves the formation of self-assembled monolayers (SAM) on atomically flat gold surfaces, but to a lesser extent in the case of AuNP where polydispersity and irregularities on the surface and curvature variations make the binding process more complex and the conclusions more difficult to generalize (7). Surface enhanced Raman spectroscopy (SERS) has proven a useful tool to study structural effects and kinetics of thiol-AuNP interactions (7, 8), although relatively large particle sizes (e.g. 50-200 nm) and aromatic thiols tend to be preferred to suit SERS optimal experimental conditions (9). Thus, we combine fluorescence and SERS as a way to generalize our results to different chemical structures and particle sizes.

While working on preparing thiolated stabilized AuNP, we have asked ourselves how long we had to wait until the derivatization was complete, so as to avoid working with nanostructures that were still undergoing significant change. A few literature studies (such as those mentioned above) address this question for specific systems, yet, much more frequent are literature contributions where the delay between thiolate derivatization and usage of the nanostructures is simply not mentioned. A study of the influence of thiolate derivatization on the catalytic reduction of 4-nitrophenol serves as a perfect example of the importance of thiolate coverage on

the catalytic performance (10). The free catalytic site density determines the activity of the material. Interestingly, considerable catalytic activity is retained even when the coverage is 90 %.

The motivation for this study is our interest in the delay between reagent mixing and completion of the S-Au derivatization process. In order to address this issue, we employed two strategies. One of these methodologies involves simple fluorescence spectroscopy. In our work, fluorescence spectroscopy is used as a tool that is suitable for different combinations of nanostructure and sensing molecules (Scheme 1). In the other approach, Raman spectroscopy is used to further support our results. While recognizing that our data contain kinetic and mechanistic information and do some simple kinetic analysis, we use a rather pragmatic approach by trying to answer this question. It is important to note that the type (particularly size) of nanoparticles and the organic structures required to optimize fluorescence and SERS measurements are different and thus the sections that follow, dealing with fluorescence and Raman spectroscopy are not directly comparable. In this case, this is an asset, as it allows us to establish the generality of the conclusions we reach in this contribution. Scheme 1 shows the molecules examined in this contribution.

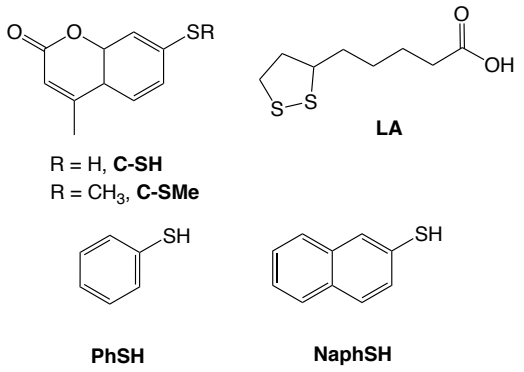

Scheme 1. Thiol compounds used in this study.

MATERIALS AND METHODS

Materials and Instrumentation: All reagents have been purchased from Sigma-Aldrich and have been used without further purification unless otherwise stated. S-methyl-7-mercapto-4-methylcoumarin (C-SMe) was synthesized as previously described (11). AuNPs were synthesized using a reported method (12) via reduction with sodium citrate. Briefly, 230 mL of a 0.3 mM aqueous solution of $HAuCl_4$ were heated up to boiling point, then 20 mL of a 39 mM solution of sodium citrate were quickly added to the solution and boiled for 2 h. The ruby-red solution obtained was kept at room temperature and properly diluted before use. Transmission electron microscopy (TEM) images were collected using a JEM-2100F FETEM (JEOL) working at an acceleration voltage of 200 kV. Steady-state absorbance and fluorescence measurements were recorded on a Cary 100 spectrophotometer and a Photon Technology International (PTI) fluorimeter, respectively. Raman spectra were recorded in a Horiba Xplora microscope configured with 532 nm (at 24 μW) and 785 nm (at 50 μW) laser lines at 100 % power. Data analyses were done using LabSpec 6 software.

Fluorescence spectroscopy measurements: Initial fluorescence testing was run to determine appropriate concentrations of 7-Mercapto-4-methylcoumarin (dimethyl sulfoxide –DMSO– solution) for fluorescence testing. Kinetic studies were performed by monitoring the fluorescence of fixed-volume AuNP solutions (~ 12 nm average diameter, 1.2 nM) in the presence of varying amounts of 7-mercapto-4-methylcoumarin; kinetic runs were followed at 430 nm (Excitation wavelength = 358 nm). In addition, fluorescence spectra were recorded by exciting 7-mercapto-4-methylcoumarin solutions before and after 1.5 h of kinetic testing.

Surface enhanced Raman spectroscopy measurements: AuNP's surface functionalization was monitored utilizing two different thiols, namely thiophenol (PhSH) and 2-Naphthalenethiol (NaphSH). Stock solutions of PhSH were prepared daily and diluted in purified 18.2 MΩ water; while stock solutions of NaphSH were prepared in EtOH and stored at 4 ºC for a maximum of one week, followed by the appropriate daily dilution in a 1:1 EtOH/Water mixture. Measurements were performed in solution upon addition of thiol into AuNP (~ 60 nm average diameter, 31 pM) solutions at given concentrations. SERS measurements were performed on AuNP solution in the presence of various thiol concentrations and recorded at the following acquisition conditions: 785 nm laser (25% power), 5s integration time, 10 accumulations per spectrum and 60 s measurement interval time. The peak areas were calculated using LabSpec software (HORIBA).

All kinetics experiments were fitted using a user-defined fitting with Kaleidagraph or Origin software.

RESULTS AND DISCUSSION

Kinetics based on fluorescence spectroscopy

In our work, fluorescence spectroscopy was used as a suitable tool to study different combinations of AuNP and various sensing molecules (Scheme 1). While analyzing the obtained data to extract kinetic and mechanistic information, we use a pragmatic approach by trying to answer the question on hand: how fast can thiols bind to the gold-nanoparticle surface?

We have found that 7-mercapto-4-methyl coumarin (C-SH) is an excellent substrate for fluorescence spectroscopy, and commercially available. Interestingly, C-SH is weakly

fluorescent as a result of non-radiative deactivation (13), attributed to the thione resonance structure contributions (Scheme 2) (11).

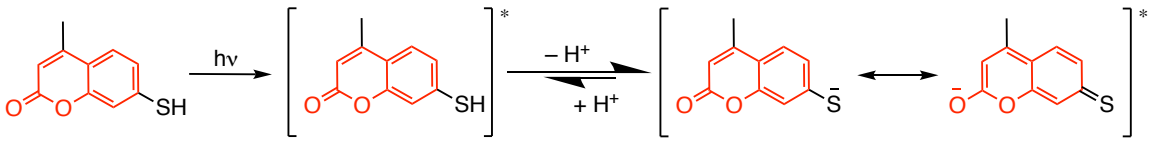

Scheme 2. Excited C-SH is prone to deprotonate and favor the thione-like resonance form (non-emissive). Notice in red the coumarin core. Adapted from Ref (11).

When the S-H bond is substituted, for example by a methyl group (C-SMe) the molecule becomes strongly fluorescent (Figure 1), despite what is expected for its hydroxy counterpart (14). Notice that Figure 1 shows that C-SMe is a much stronger emitter than C-SH, typically 20-100 times. We have explained this effect in an earlier contribution using Scheme 2 to rationalize the effect (11). Additionally, a modest fluorescence enhancement due to the presence of AuNP is detected, in contrast to typical plasmonic enhancements reported to be an order of magnitude larger (15). It is known that while proximity enhances the signal, surface contact results in emission quenching; the experimental observation depends on the balance of these effects, on the system as well as on the experimental conditions (15, 16).

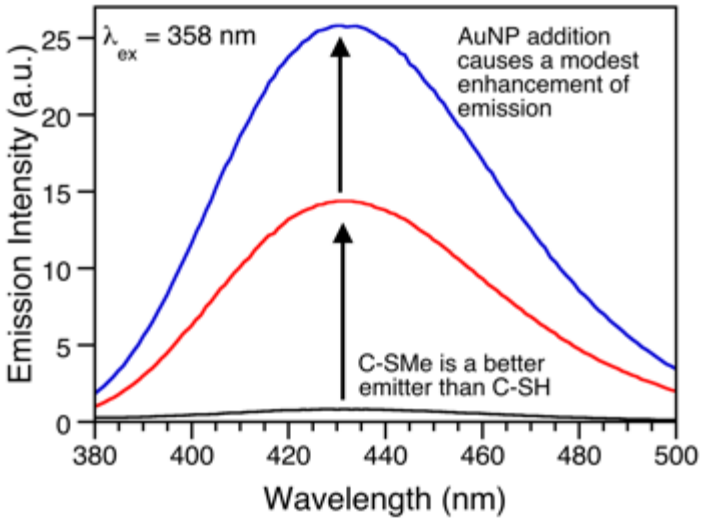

Figure 1. Emission spectra of 0.52 μM of C-SH (black), 0.052 μM of C-SMe (red) and the C-SMe sample after addition of 1.2 nM AuNP (blue) and a 5 min incubation. All in 10% DMSO:H_2O.

The addition of C-SH to the gold surface leads to the displacement of citrate and the formation of thiolate bonds (12), Scheme 3, with concomitant spectral changes in the AuNP region (~530 nm) and the appearance of the coumarin absorption band in the 360 nm region, Figure 2. Thus, the S-H bond can be eliminated by coordination to the gold surface (Scheme 3), which is typically the key step in AuNP derivatization. With this in mind, we decided to design a simple way to determine how fast the interaction between thiols and AuNP surface can take place, using C-SH as a probe. Thus, we expect the thione-like resonance form of C-SH to be less favored as the thiol moiety is engaged in binding to the AuNPs surface, increasing the fluorescence emission of the coumarin. The increase in fluorescence signal can account then for the formal interaction between the thiol moiety and the Au surface, and help reveal kinetic information about the process. While fluorescence quenching is expected, when fluorophores sit right on the surface of plasmonic materials such as AuNP, the experimental balance in this case is a moderate (but readily detectable) fluorescence enhancement (16). Thus, the use of fluorescence

enhancement provides a novel approach to monitor reactivity with the gold plasmonic surface. The changes in Figure 2 are attributed to modifications on the surface of the AuNPs, as well as changes in the dielectric media, as a consequence of the presence of C-SH. Changes produced by the addition of the different solvent were ruled out. Pure DMSO was added to AuNP under the same conditions and no deviations in the absorption spectrum were detected.

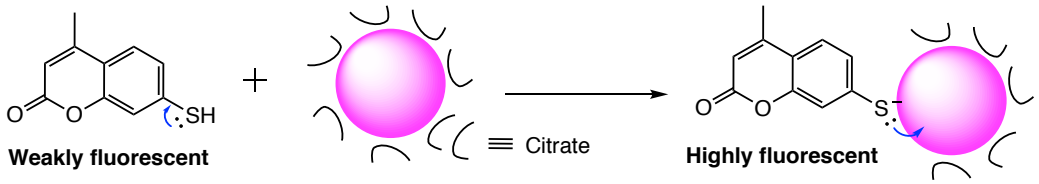

Scheme 3. The formation of strong thiolate bonds causes the displacement of citrate from the gold surface.

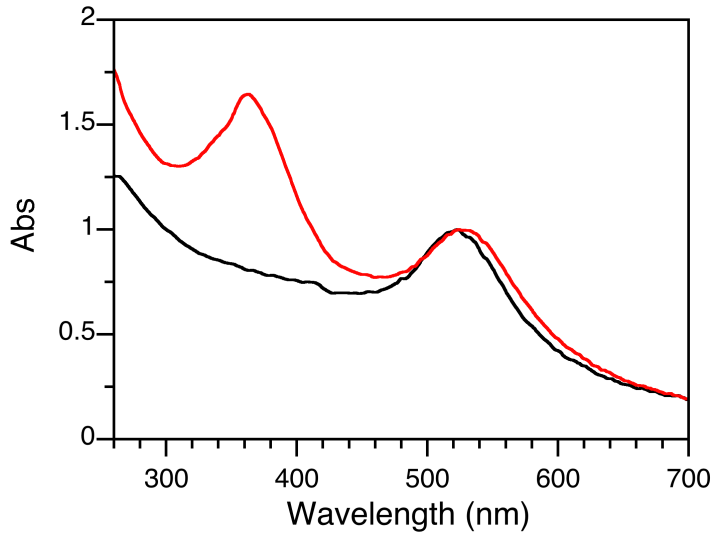

Figure 2. Normalized absorption spectra of AuNPs in the absence (black) and in the presence (red) of 160 µM of C-SH. Notice the plasmon band maximum for AuNP shifts from 522 nm to 528 nm.

AuNP used for fluorescence spectroscopy (Figure 3) have an average size of 12 nm, significantly smaller than those used for Raman spectroscopy (~60 nm, *vide infra*). Particles were initially tested at two different AuNP concentrations: 2.4 and 1.2 nM (calculated as previously reported

(16)). Figure 4 shows how the emission at 440 nm, corresponding to C-SH, increases after mixing with AuNP solution. Notice that while essentially the same rate constants are obtained, diluted AuNP solutions reach higher fluorescence intensities, more likely due to better light penetration and minimal light re-absorption.

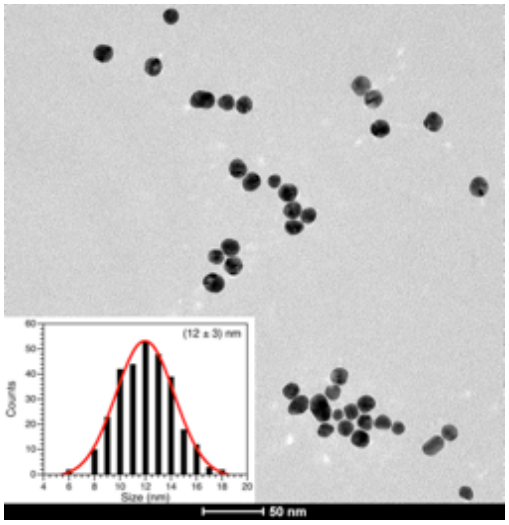

Figure 3. HR-TEM images of the AuNP used for fluorescence experiments and (inset) particle size distribution for one of the two batches on AuNP used.

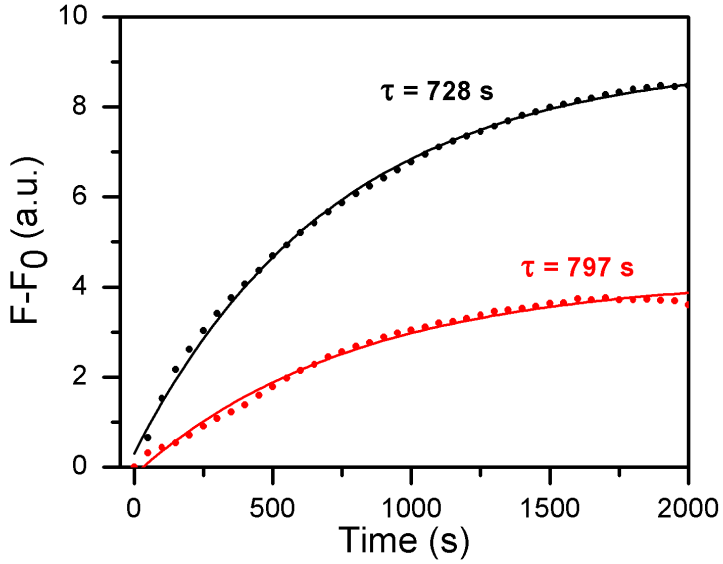

Figure 4. Fluorescence intensity change ($F-F_0$) monitored at 430 nm (λ_{ex} = 358 nm) versus time for 4 μM of C-SH in the presence of 1.2 nM (black) and 2.4 nM (red) of AuNP. Fit to a first-order exponential growth model (solid line). Notice same rate constant values, k_{obs}, are obtained for both NP concentrations.

Figure 4 clearly shows that changes in the AuNP concentration led to unusual effects (such as more signal with less AuNP) that while readily explained on a qualitative basis pose serious challenges for quantification. Thus, most of the experiments that follow center on kinetic studies where thiol concentrations are changed while maintaining the AuNP concentration constant. Representative results are shown in Figure 5, where C-SH was added in concentrations ranging from 1 to 6 μM and monitored for 2000 s. Note that only the emission growth component of the signal is displayed in Figure 5, as C-SH, while weak is somewhat emissive (see Figure 1). This emission is probably slightly enhanced by non-reactive initial interaction with the gold surface. An example of the uncorrected traces is shown as an inset in Figure 5. A simple visual inspection of Figure 5 shows that about 30 minutes is required for 90% of the reaction to take place.

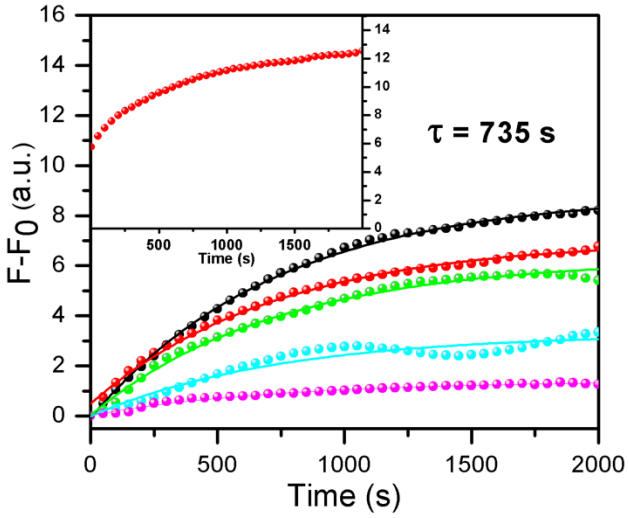

Figure 5. Fluorescence intensity for different concentrations of C-SH added to 1.2 nM of AuNP and monitored at 430 nm versus time. The fitting lines shown have been calculated by global analysis of the reaction kinetics. Concentration of C-SH from the bottom to the top: 1, 2, 3, 4, 6 μM. Inset: uncorrected trace for 4 μM solution.

The surface of each AuNP must present sites with different reactivity, further, the material size distribution is not monodisperse, as Figure 3 shows. Under these conditions, it is remarkable that the plots of Figure 5 can be reasonably fitted with a monoexponential growth, in other words, they follow excellent Langmuir-type first order kinetics. In fact, it was possible to use a kinetic global fitting approach to fit the data in Figure 5 using equation (1).

$$A = A_0(1 - e^{-kt}) \qquad (1)$$

where k is the observed rate constant for the growth of A (enhanced Raman or emission signal) and is equal to the inverse of the lifetime ($1/\tau$). We obtain k as the value that minimizes the mean squared error between the fitted and the observed kinetic curves with different values of A_0.

Global kinetic analysis of Figure 5 yields a lifetime (τ) of 735 s. Considering that three lifetimes corresponds to 95% completion, the visual estimate of 30 minutes mentioned above appears quite reasonable. Beyond a single lifetime or rate constant, global analysis also yields a projected plateau value for the signal (A_0). These values were recorded and plotted against concentration in Figure 6. The plot reaches a plateau that implies the mercaptan and not the AuNP is the likely limiting reagent in this system. At the highest C-SH concentration, this corresponds to ~3300 thiolate bonds per nanoparticle.

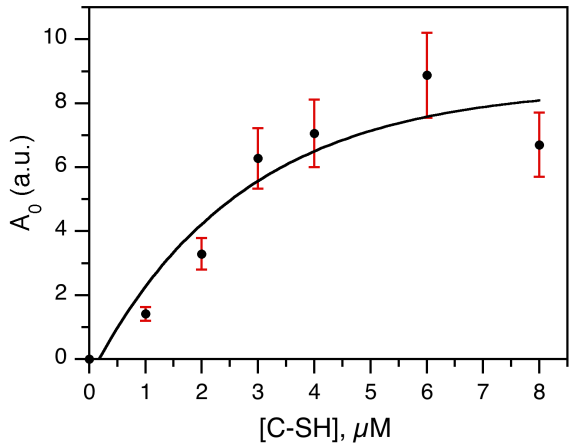

Figure 6. Fluorescence intensity change (A_0) determined from the calculated plateau in figure 5 plotted as a function of the C-SH concentration. Errors estimated as 15%.

In order to prove the reproducibility of this methodology, a second batch of AuNP (~17 nm, see SI) was prepared and the same type of kinetics were evaluated. Figure 7 shows the kinetic traces obtained.

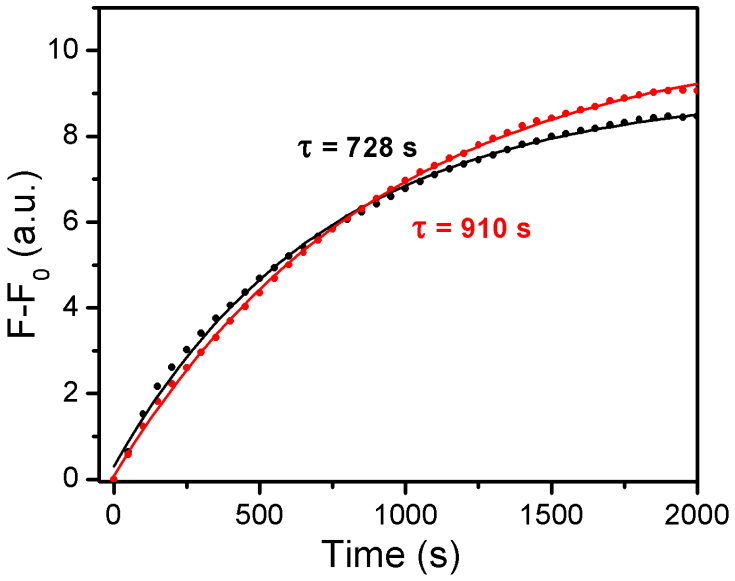

Figure 7. Fluorescence intensity for 4 μM of C-SH added to 1.2 nM of AuNP batch 1 (black) and batch 2 (red) and monitored at 430 nm versus time. The fitting lines shown have been calculated by first exponential growth kinetics (eq. 1).

The lifetime values of 767, 638 and 660 s, derived from single curve analysis (Figure 7) and global analysis (Figure 5) illustrate the type of reproducibility that can be expected in these systems as the sample batch and/or type of analysis is changed.

220

Kinetics based on Raman spectroscopy

Surface enhanced Raman spectroscopy (SERS) is also an important and complementary tool in determining the reactivity of the S-H bond towards the gold surface. The best suited molecules for SERS differ from those preferred for fluorescent studies, and thus, non-fluorescent or weakly

225 fluorescent aromatic molecules, such as PhSH and NaphSH (see Scheme 1) were the choices for these studies. AuNP concentration was also optimized in order to have greater Raman signal enhancement. Further, larger particles are optimal for SERS, and thus citrate-covered 65 nm AuNP were preferred. The Raman spectra for PhSH and NaphSH are shown in Figure 8; notice in the inset that in addition to polydispersity, the sample shows some polymorphism.

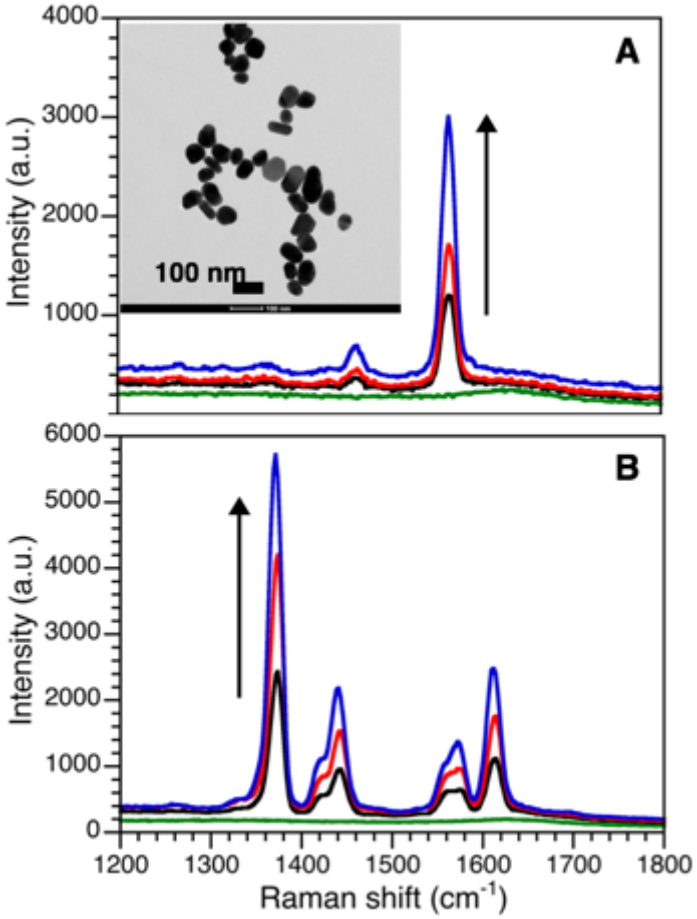

Figure 8. Raman spectra for thiol-modified AuNP obtained with different concentrations of thiol after 30 min of mixing. (A): PhSH at 0 (green), 60 nM (black), 100 nM (red) and 200 nM (blue). (B): NaphSH at 0 (green), 50 nM (black), 100 nM (red) and 200 nM (blue). In both cases, the Raman signal increases with concentration

In the case of PhSH, Raman peaks at 408 (C-S), 1067 (C-H) and 1565cm^{-1} (C=C) could be monitored to observe the enhancement that results from binding at the AuNP surface. In our case, we found the 1565 cm^{-1} peak to be the most convenient for PhSH (Figure 9). Likewise, we followed the addition of NaphSH monitoring the area of the C=C peak at 1370 cm^{-1} (Figure 10).

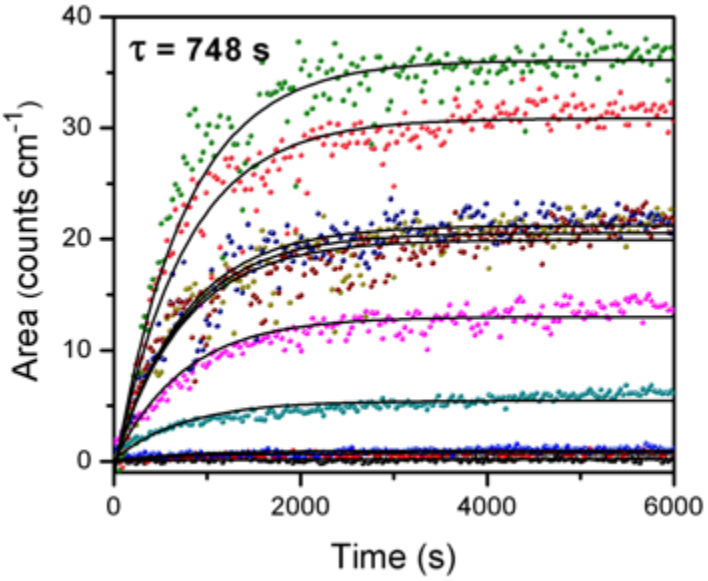

Figure 9. Kinetics experiment for the AuNP surface modification with different concentrations of PhSH in water added to 31 pM AuNP solution, monitoring the area of the C=C peak at 1565 cm^{-1} and fitted using global analysis. [PhSH] from the bottom to the top: 20, 40, 50, 55, 60, 80, 100, 140, 200, 220 nM.

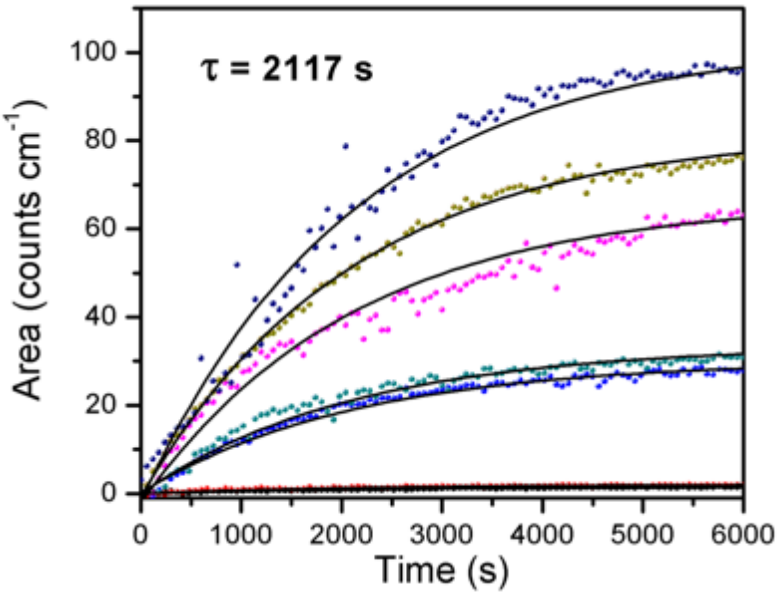

Figure 10. Kinetics experiment for the AuNP surface modification with different concentrations of NaphSH in water added to 31 pM AuNP solution, monitoring the area of the C=C peak at 1370 cm^{-1} and fitted using global analysis. [NaphSH] from the bottom to the top: 20, 40, 50, 60, 90, 100, 200 nM.

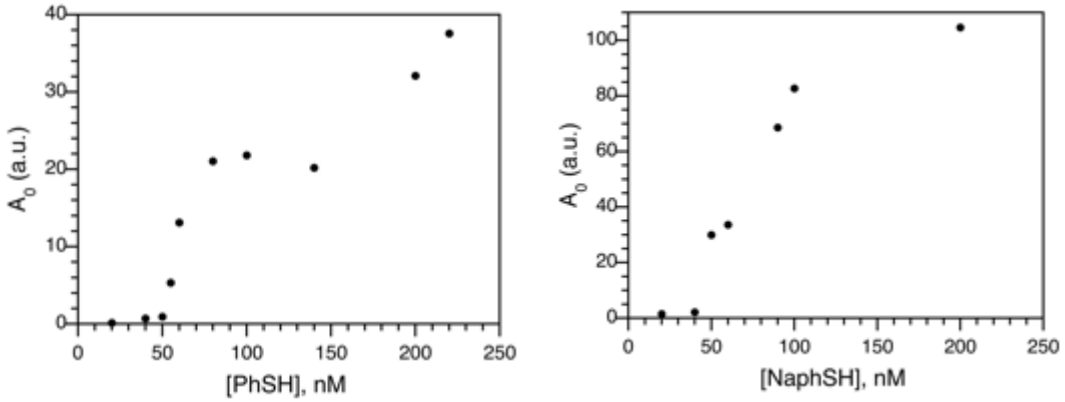

Figure 11. Raman area change (A_0) determined from the calculated plateau in figure 8 and 9 plotted as a function of the thiol concentration. Notice the saturation of the plot up to ~ 3200 molecules of thiol per AuNP, corresponding to a concentration of 100 nM of thiol per 31 pM AuNP solution.

Competition binding by lipoic acid

The case of lipoic acid (LA) is particularly interesting, as its behavior should mimic disulfides, however –due to its cyclic structure– once LA binds to the gold surface produces more stable molecular arrangements because of the formation of two S-Au bonds. (17). We have designed two types of fluorescence experiments where LA and C-SH compete for the gold surface. In the first one equimolar concentrations of both are added simultaneously to a AuNP solution. As shown in Figure 12, the presence of LA has virtually no effect on the growth of the fluorescence of C-SH from the gold-bonded mercaptocoumarin. This result implies that for C-SH and LA, thiols are more reactive than disulfides, likely because S-S bond breaking is required for LA. In the second type of experiments the reagents are exactly the same, however, in this case the AuNP were pre-incubated at the same concentration of LA for 24 h, prior to addition of C-SH. These results are also presented in Figure 12, and show a smaller and somewhat slower fluorescence growth, illustrating that LA has bonded to the gold surface thus reducing the number of active sites available for C-SH reaction.

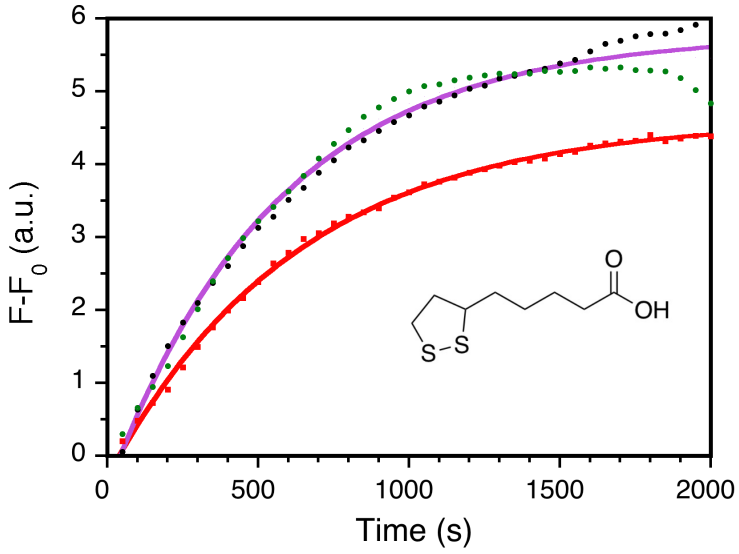

Figure 12. Fluorescence intensity change ($F-F_0$) monitored at 430 nm versus time from solution of 1.2 nM of AuNP after addition of 4 µM C-SH (black), 4 µM C-SH and 4 µM LA (green) and 4 µM C-SH added to a AuNP solution previously incubated for 24 h with 4 µM LA (red). The purple line fits simultaneously black and green data (differences within the experimental error).

Thus, the competition of C-SH with LA shows that thiols are far more reactive than disulfide, as adding LA as a competitive reagent does not affect the growth curve giving a growth lifetime of 560 ± 70 s. On the other hand, if AuNP are pre-incubated overnight with LA, the disulfide can bind to the surface (frequently described as two-footed binding) and protect it from the thiols attack. This results in a lifetime of 620 ± 70 s and the final fluorescence is only 78% of that achieved without pre-incubation. With pre-incubation less sites are available, but those that remain available are within experimental errors just as reactive as those encountered on a fresh surface. Overall LA binding must be about ten times slower than thiol reaction, thus needing overnight incubation to make a real difference in C-SH binding.

CONCLUSION

These results prove the reactivity of several thiols occurs within the same timescale, however disulfides (such as LA) react much more slowly. To answer the title question, we recommend one to two hour wait for thiol binding to be essentially complete, while for disulfides, overnight incubation is recommended. Any "ready-mix" strategy is bound to lead to results obtained while the formation of thiolate bonds was still in progress.

ACKNOWLEDGMENTS

Thanks are due to the Discovery program from Natural Sciences and Engineering Research Council of Canada, the Canada Research Chairs Program, the Canada Foundation for Innovation and the Canadian Genome Program.

SUPPLEMENTARY MATERIALS

Supporting materials include details of the calculation of nanoparticle concentrations and additional TEM images.

REFERENCES

1. Hakkinen, H. (2012) The gold-sulfur interface at the nanoscale. *Nat. Chem.* **4,** 443-455.
2. Pensa, E., E. Cortes, G. Corthey, P. Carro, C. Vericat, M. H. Fonticelli, G. Benitez, A. A. Rubert and R. C. Salvarezza (2012) The Chemistry of the Sulfur-Gold Interface: In Search of a Unified Model. *Acc. Chem. Res.* **45,** 1183-1192.
3. Goldmann, C., R. Lazzari, X. Paquez, C. Boissiere, F. Ribot, C. Sanchez, C. Chaneac and D. Portehault (2015) Charge Transfer at Hybrid Interfaces: Plasmonics of Aromatic Thiol-Capped Gold Nanoparticles. *ACS Nano* **9,** 7572-7582.
4. Reimers, J. R., M. J. Ford, S. M. Marcuccio, J. Ulstrup and N. S. Hush (2017) Competition of van der Waals and chemical forces on gold–sulfur surfaces and nanoparticles. *Nat. Rev. Chem.* **1,** 0017.

5. Stamplecoskie, K. G., G. Yousefalizadeh, L. Gozdzialski and H. Ramsay (2018) Photovoltaics as an Experimental Tool for Determining Frontier Orbital Energies and Photocatalytic Activity of Thiol Protected Gold Clusters. *J Phys. Chem. C* **122,** 13738-13744.
6. Yousefalizadeh, G. and K. G. Stamplecoskie (2018) Norrish type I photochemistry as a powerful tool in the isolation of thiol protected Au25SR18 clusters. *J. Photochem. Photobiol., A* **353,** 251-254.
7. Villarreal, E., G. F. G. Li, Q. F. Zhang, X. Q. Fu and H. Wang (2017) Nanoscale Surface Curvature Effects on Ligand-Nanoparticle Interactions: A Plasmon-Enhanced Spectroscopic Study of Thiolated Ligand Adsorption, Desorption, and Exchange on Gold Nanoparticles. *Nano Lett.* **17,** 4443-4452.
8. DeVetter, B. M., P. Mukherjee, C. J. Murphy and R. Bhargava (2015) Measuring binding kinetics of aromatic thiolated molecules with nanoparticles via surface-enhanced Raman spectroscopy. *Nanoscale* **7,** 8766-8775.
9. Stamplecoskie, K. G., J. C. Scaiano, V. S. Tiwari and H. Anis (2011) Optimal Size of Silver Nanoparticles for Surface-Enhanced Raman Spectroscopy. *J Phys. Chem. C* **115,** 1403-1409.
10. Ansar, S. M. and C. L. Kitchens (2016) Impact of Gold Nanoparticle Stabilizing Ligands on the Colloidal Catalytic Reduction of 4-Nitrophenol. *ACS Catal.* **6,** 5553-5560.
11. Lanterna, A. E., M. Gonzalez-Bejar, M. Frenette and J. C. Scaiano (2017) Photophysics of 7-mercapto-4-methylcoumarin and derivatives: complementary fluorescence behaviour to 7-hydroxycoumarins. *Photochem. Photobiol. Sci.* **16,** 1284-1289.
12. Vanegas, J. P., J. C. Scaiano and A. E. Lanterna (2017) Thiol-Stabilized Gold Nanoparticles: New Ways To Displace Thiol Layers Using Yttrium or Lanthanide Chlorides. *Langmuir* **33,** 12149-12154.
13. Gonzalez-Bejar, M., M. Frenette, L. Jorge and J. C. Scaiano (2009) 7-Mercapto-4-methylcoumarin as a reporter of thiol binding to the CdSe quantum dot surface. *Chem. Commun.*, 3202-3204.
14. Demelo, J. S. S., R. S. Becker and A. L. Macanita (1994) Photophysical Behavior of Coumarins as a Function of Substitution and Solvent - Experimental-Evidence for the Existence of a Lowest Lying $^1(n,\pi^*)$ State. *J Phys. Chem.* **98,** 6054-6058.
15. Anger, P., P. Bharadwaj and L. Novotny (2006) Enhancement and quenching of single-molecule fluorescence. *Phys. Rev. Lett.* **96**.
16. Pacioni, N. L., M. Gonzalez-Bejar, E. Alarcon, K. L. McGilvray and J. C. Scaiano (2010) Surface Plasmons Control the Dynamics of Excited Triplet States in the Presence of Gold Nanoparticles. *J. Am. Chem. Soc.* **132,** 6298-6299.
17. Asadirad, A. M., Z. Erno and N. R. Branda (2013) Photothermal release of singlet oxygen from gold nanoparticles. *Chem. Commun.* **49,** 5639-5641.